









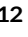

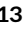






Clinical variability at the mild end of *BRAT1*-related spectrum: Evidence from two families with genotype–phenotype discordance

Sara Nuovo¹ | Valentina Baglioni¹ | Roberta De Mori²  | Silvia Tardivo²  |
Caterina Caputi¹  | Monia Ginevrino^{3,4}  | Alessia Micalizzi³  | Laura Masuelli⁵  |
Giulia Federici⁶  | Antonella Casella^{7,8}  | Elisa Loreface⁹  | Danila Anello¹⁰ |
Manuela Tolve⁵  | Donatella Farini^{11,12}  | Enrico Bertini¹³  | Ginevra Zanni¹³  |
Lorena Travaglini¹³  | Gessica Vasco¹⁴  | Claudio Sette^{12,15}  | Carla Carducci⁵  |
Enza M. Valente^{7,8} | Vincenzo Leuzzi¹

¹Department of Human Neuroscience, Sapienza University of Rome, Roma, Italy

²Neurogenetics Unit, IRCCS Santa Lucia Foundation, Roma, Italy

³Translational Cytogenomics Research Unit, Bambino Gesù Children's Hospital, IRCCS, Roma, Italy

⁴Istituto di Medicina Genomica, Università Cattolica del Sacro Cuore, Fondazione Policlinico Universitario "A. Gemelli" IRCCS, Roma, Italy

⁵Department of Experimental Medicine, Sapienza University of Rome, Roma, Italy

⁶Unit of Cellular Networks and Molecular Therapeutic Targets, IRCCS – Regina Elena National Cancer Institute, Roma, Italy

⁷Department of Molecular Medicine, University of Pavia, Pavia, Italy

⁸Neurogenetics Research Centre, IRCCS Mondino Foundation, Pavia, Italy

⁹Department of Molecular Medicine, Sapienza University of Rome, Roma, Italy

¹⁰Department of Medical and Surgery Sciences, Catholic University of the Sacred Heart, Roma, Italy

¹¹Department of Biomedicine and Prevention, University of Rome Tor Vergata, Roma, Italy

¹²Laboratory of Neuroembryology, IRCCS Santa Lucia Foundation, Roma, Italy

¹³Unit of Neuromuscular and Neurodegenerative Diseases, Department of Neuroscience and Neurorehabilitation, IRCCS Bambino Gesù Children's Hospital, Roma, Italy

¹⁴Neuroscience and Neurorehabilitation Department, MARlab, IRCCS Bambino Gesù Children's Hospital, Roma, Italy

¹⁵Section of Human Anatomy, Department of Neuroscience, Catholic University of the Sacred Heart, Roma, Italy

Correspondence

Vincenzo Leuzzi, Department of Human Neuroscience, Sapienza University of Rome, Via dei Sabelli 108, 00185 Roma, Italy.
Email: vincenzo.leuzzi@uniroma1.it

Funding information

H2020 European Research Council, Grant/Award Number: Starting Grant 260888 to EMV; Fondazione Pierfranco e Luisa Mariani, Grant/Award Number: PADAPORT project to EMV; Italian Ministry of Health, Grant/Award Numbers: Ricerca Corrente 2020

Abstract

Biallelic mutations in the *BRAT1* gene, encoding BRCA1-associated ATM activator 1, result in variable phenotypes, from rigidity and multifocal seizure syndrome, lethal neonatal to neurodevelopmental disorder, and cerebellar atrophy with or without seizures, without obvious genotype–phenotype associations. We describe two families at the mildest end of the spectrum, differing in clinical presentation despite a common genotype at the *BRAT1* locus. Two siblings displayed nonprogressive congenital ataxia and shrunken cerebellum on magnetic resonance imaging. A third unrelated patient showed normal neurodevelopment, adolescence-onset seizures, and ataxia, shrunken cerebellum, and

Sara Nuovo and Valentina Baglioni contributed equally to this study.

Enza M. Valente and Vincenzo Leuzzi are senior authors.

to IRCCS Mondino, Ricerca Finalizzata NET-2013-02356160 to EB, EMV

ultrastructural abnormalities on skin biopsy, representing the mildest form of NEDCAS hitherto described. Exome sequencing identified the c.638dup and the novel c.1395G>A *BRAT1* variants, the latter causing exon 10 skipings. The p53-MCL test revealed normal ATM kinase activity. Our findings broaden the allelic and clinical spectrum of *BRAT1*-related disease, which should be suspected in presence of nonprogressive cerebellar signs, even without a neurodevelopmental disorder.

KEYWORDS

BRAT1, NEDCAS, nonprogressive congenital ataxia, phenotypic discordance, splicing variant

BRAT1 gene (MIM# 614506) encodes BRCA1-associated ATM activator 1, which interacts with the tumor suppressors BRCA1 and ATM, playing an important role in the DNA damage response (DDR) (Aglipay et al., 2006). Moreover, it is involved in p53-mediated apoptosis, cellular growth signaling, and mitochondrial homeostasis (Aglipay et al., 2006; So & Ouchi, 2014). Recessive *BRAT1* mutations were originally reported to cause rigidity and multifocal seizure syndrome, lethal neonatal (RMFSL, MIM# 614498), a rare congenital disorder characterized by microcephaly, hypertonia, autonomic instability, and intractable seizure, leading to death in the first 2 years of life (Burgess et al., 2019; Colak et al., 2020; Pourahmadiyan et al., 2020; Scheffer et al., 2020; Valence et al., 2019; Van Ommeren et al., 2018). Brain imaging was highly variable, ranging from normal findings to global atrophy (Srivastava et al., 2016). Few patients have a milder presentation known as neurodevelopmental disorder with cerebellar atrophy with or without seizures (NEDCAS; MIM# 618056), characterized by prolonged survival and a variable degree of intellectual disability (ID) and cerebellar involvement (Fernández-Jaén et al., 2016; Hanes et al., 2015; Mahjoub et al., 2019; Mundy et al., 2016; Oatts et al., 2017; Srivastava et al., 2016; Valence et al., 2019). Smith et al. (2016) suggested that the observed phenotypic differences might relate to the functional consequences of the identified mutations, as variants leading to premature protein termination were more frequently associated with the severe form of the disease. Nevertheless, genotype-phenotype associations are not fully elucidated. Herein, we report three novel patients from two unrelated Italian families, who showed a highly variable clinical presentation resulting from an identical genotype at *BRAT1* locus. The two siblings from the first family displayed nonprogressive congenital ataxia (NPCA) with ID. In contrast, the third patient showed seizures, mild functioning decline, and fluctuating ataxia with onset in adolescence, associated with atypical ultrastructural findings in skin biopsy, representing the mildest case described so far. Our findings broaden the allelic and clinical spectrum of *BRAT1*-related disease and provide new insights into disease pathogenesis.

Patients were examined at Bambino Gesù Children's Hospital and University Hospital "Policlinico Umberto I." Family A was enrolled in a multicentric project aimed at identifying the genetic basis of cerebellar and brainstem congenital defects, whereas Family B was investigated in a diagnostic setting. Written informed consent was obtained from participants (approval of the University of Pavia Ethics Committee, Prot.20180077857/12-09-2018).

Ultrastructural analysis was performed on a 3-mm punch skin biopsy, fixed in 2.5% glutaraldehyde in 1X phosphate-buffered saline pH 7.4, and then processed for transmission electron microscopy (Morgagni 268D) following routine procedures (Mastrangelo et al., 2019).

For Family A, whole exome sequencing was performed on genomic DNA of both affected brothers. Libraries were prepared through SureSelectXT Clinical Research Exome V1 protocol (Agilent Technologies) and ran on a HiSeq 2500 (Illumina) sequencer. For Family B, clinical exome sequencing was performed on proband's DNA by using TruSightOne Kit (Illumina Nextera) on a MiseqDx (Illumina) platform. Sequencing data were analyzed as reported (Ginevrino et al., 2020). Validation and familiar segregation of candidate variants were performed by Sanger. Variants were submitted to the Leiden open variation database (<http://www.LOVD.nl>).

RNA was extracted using the Total RNA Mini Kit (Geneaid) and retrotranscribed with PrimeScript™ RT Reagent Kit (Takara). Complementary DNA (cDNA) of *BRAT1* was polymerase chain reaction (PCR) amplified and visualized on a 2% agarose gel. Fragments isolated through electrophoresis were recovered by Zymoclean™ Gel DNA Recovery Kit (Zymo Research) and sequenced. cDNAs were analyzed by real-time PCR using SYBR® Premix Ex Taq II (Takara) on the Light-Cycler® 480 Instrument II (Roche Life Science) to evaluate the expression levels of mutated and wild-type (WT) transcripts. The relative expression was calculated using the method (primer sequences provided in Table S1).

The DNA fragment encompassing exon 9–11 genomic region of the *BRAT1* gene was amplified by the Phusion Hot Start High-Fidelity DNA Polymerase (Thermo Fisher Scientific) from human genomic DNA and cloned into the HindIII-NotI restriction sites of pCDNA3.1(+) vector. For cloning the *BRAT1*G>A mutant (identified in the present study) and the previously reported *BRAT1*G>C mutant (Burgess et al., 2019; Van Ommeren et al., 2018), site-directed mutagenesis was performed using the QuikChangeR II Site-Directed Mutagenesis Kit (Stratagene). Minigenes vectors were sequenced (Eurofins Genomics). HEK293T cells cultured with Dulbecco's modified Eagle's medium (Sigma-Aldrich) supplemented with 10% fetal bovine serum (Euroclone) were transfected with either *BRAT1* WT or mutant minigene vectors using Lipofectamine 2000 (Invitrogen). After 24 h, cells were collected and total RNA was extracted using TRIzol (Invitrogen), digested with RNase-free DNase (Roche) and

retrotranscribed using Moloney murine leukemia virus reverse transcriptase (Promega). PCR reactions for splicing analysis were performed using GoTaq (Promega). Samples were separated on a 2.5% agarose gel and bands intensity was quantified with ImageJ (<https://imagej.net/Fiji>) (primer sequences provided in Table S1).

Patients' fibroblasts were lysed in radioimmunoprecipitation assay buffer containing protease and phosphatase inhibitors and protein extracts were quantified by Bradford assay. Equivalent amounts of lysates were resolved by electrophoresis through 8%–16% Mini-PROTEAN TGX Gel (Bio-Rad) and probed with primary anti-BRAT1 (GeneTex) and anti-GAPDH (Sigma-Aldrich).

Possible consequences of the *BRAT1* variants on ATM activity were investigated through the p53-MCL test, based on the ATM ability to phosphorylate p53 at serine 15 and promote p53 mitotic centrosomal localization (Prodosmo et al., 2013).

The index patient of Family A was a 15-year-old boy, first son of healthy nonconsanguineous parents. He was included in our research project at the age of 7 due to neurodevelopmental delay, ID, and ataxia. Neurological assessment showed moderate ataxia with need of special walker, generalized hypotonia, bilateral pes planus, severe dysarthria, strabismus, and nystagmus. His neuropsychological profile was characterized by mild-moderate ID (based on clinical observation) and behavioral problem treated with antipsychotic medication and poor linguistic skills. At 6 years, a moderate-severe sensorineural hearing loss was detected by impedentiometry, brainstem auditory evoked potentials and otoacoustic emissions. In addition, he also suffered from periodic fever, aphthous stomatitis, pharyngitis, and adenitis. A brain magnetic resonance imaging (MRI), performed at 1.5 years of age, revealed a mildly shrunken cerebellum with enlarged interfolial spaces, without other abnormalities (Figure 1a–c). The clinical course was stable, with mild improvement in relational, motor praxis, and linguistic skills since the age of 6. Brain imaging repeated 5 years later, remained unmodified (Figure 1d–f). The younger brother, currently aged 10 years, had a similar presentation (characterized by neurodevelopmental delay, ataxia, hypotonia, dysarthria, and nystagmus), a mild ID, and an attenuated clinical course, without strabismus, hearing loss, and behavioral problems. Brain imaging at 1.5 years revealed widened cerebellar interfolial spaces (Figure 1g–i).

The proband of Family B, an 18-year-old girl, was the first child of nonconsanguineous parents. She was born at term by vaginal delivery, presenting with nuchal cord-related dystocia (Apgar scores 5, 8, and 10). Postnatal neurological examination, developmental steps, and auxological parameters were normal. She had a regular education without any obvious learning difficulties till age 13 years, when a decline in scholar performance was observed, with particular impairments in memory and attention. The girl was first referred to a neurologist at the age of 14, after experiencing a tonic-clonic seizure. No specific factors leading to the onset of manifestations have been identified. On examination, she displayed mild daily fluctuating ataxia, distal tremor, and bradykinesia. A standardized IQ evaluation was performed for the first time at 14 years of age, revealing a borderline intellectual functioning (IQ 73 Wechsler scale) that remained stable over time. Moreover, diffuse sharp-and-wave complexes on electroencephalogram were observed.

MRI and magnetic resonance spectroscopy (MRS) showed a shrunken cerebellum with reduction of the *N*-acetyl aspartate peak (suggesting neuronal depletion), without progression over time (Figure 1j–n). Further seizures were characterized by staring spells and paroxysmal blinking. There were not specific triggers for seizures onset, neither in the patient history nor at the electroencephalogram activation tests (hyperpnea, intermittent photic stimulation). Several antiepileptic drugs (including valproic acid, levetiracetam, and lamotrigine) were ineffective in a complete control of seizures. Clinical conditions remained stable in the following years. The patient successfully completed high school and is currently attending the first year of university. During the diagnostic work-up, a skin biopsy was performed to rule out neuronal ceroid lipofuscinoses (due to the presence of juvenile-onset seizures, cognitive, and motor impairment). The ultrastructural analysis showed double-membrane bound granular and osmiophilic inclusions in the cytoplasm of dermal fibroblasts and myelinated fibers, compatible with atypical mitochondria or autophagosomes (Figure 1o–t).

Next-generation sequencing identified in all three patients the c.638dup, p.(Val214GlyfsTer189) frameshift variant and the c.1395G>A, p.(Thr465=) synonymous variant in the *BRAT1* gene (RefSeq NM_152743.3, NP_689956.2), each inherited from a healthy parent (Figure 1u,v). A comprehensive list of rare genomic variants identified in Family A and B through molecular testing is provided in Tables S2 and S3, respectively. The c.638dup variant (rs730880324) has been originally described in RMFSL (Puffenberger et al., 2012). Conversely, the c.1395G>A variant (rs201855243), involving the last nucleotide of exon 10, is reported with extremely low frequency in population databases (0.007% in exome variant server and 0.002% in Genome Aggregation Database) and has not been previously associated with disease. The synonymous substitution results in an alternatively spliced isoform which lacks the 73-bp-long exon 10 and contains a premature stop codon (p.(Pro442SerfsTer23), NP_689956.2) (Figure 2a–c). The splicing assay performed in HEK293T cells transfected with the WT minigene identified two *BRAT1* transcripts: the predominant full-length and the less expressed shorter isoform corresponding to the skipping of exon 10. Introduction of the G>A mutation in the minigene caused complete skipping of exon 10, confirming that the synonymous variant disrupts the 5' splice site and impairs splicing of the exon (Figure 2d,e). The same result was obtained with the G>C mutant minigene, investigating the impact on splicing of the previously reported c.1395G>C synonymous variant (Burgess et al., 2019; Van Ommeren et al., 2018).

BRAT1 messenger RNA (mRNA) levels were quantified through quantitative reverse transcription (qRT)-PCR by using primers discriminating the full-length and the skipped transcript. As shown in Figure 2f and Figure S1, patients maintain the expression of the full-length form, although at lower levels than a healthy control and both parents. On the other hand, mRNA levels corresponding to the skipped transcript are increased in all subjects with the synonymous variant, when compared with a healthy control or with the parent displaying the c.638dup variant.

Since the full-length transcript detected through qRT-PCR can be generated from both the WT allele and the mutated c.638dup allele, the expression of endogenous WT *BRAT1* protein was unequivocally

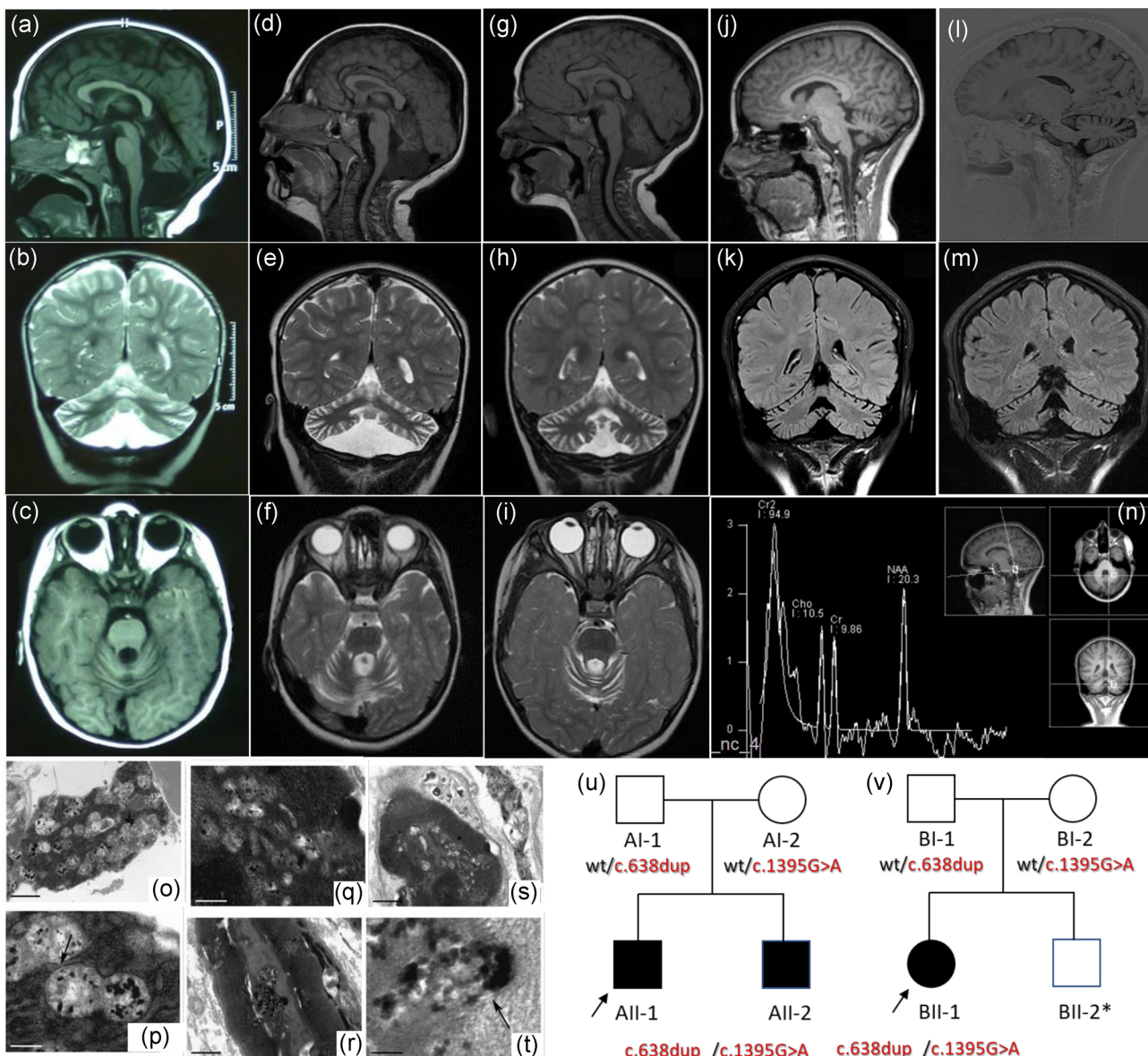


FIGURE 1 Phenotypic traits and genetic characterization of patients. Sagittal T1-, coronal T2-, and axial T1-weighted images of patient AII-1 at the age of 1.5 (a–c) and 6.5 years (d–f), showing global cerebellar hypoplasia and enlarged interfolial spaces without progression over time; sagittal T1-, coronal T2-, and axial T2-weighted images of patient AII-2 at the age of 1.5 years (g–i), revealing marked enlargement of cerebellar interfolial spaces; sagittal and coronal T1-weighted images of patient BII-1 at the age of 14 (j, k) and 17 years (l, m), showing a stable appearance characterized by widened cerebellar interfolial spaces; MR spectroscopy of patient BII-1 at the age of 14 years (n), displaying a reduction of the *N*-acetyl aspartate peak; ultrastructural analysis of skin biopsy, revealing osmiophilic granular inclusions in dermal fibroblasts (o, p) and in myelinated fibers (q–t) (arrows indicate double membranes surrounding osmiophilic granular inclusions; bars correspond to 500 nm in (o, r, s) and 200 nm in (p, q, t); pedigree of Family A (u) and Family B (v) and segregation analysis of *BRAT1* variants (filled symbols represent affected subjects; *not-tested). MR, magnetic resonance

investigated by Western blotting in fibroblasts from one patient. Results show that WT mRNA effectively goes under translation, originating WT *BRAT1* protein (Figure 2g). Interestingly, two additional bands of lower molecular weight were detected in patient's fibroblasts, that might represent the two mutated proteins derived from *BRAT1* variants.

Lastly, the p53-MCL test detected a centrosomal localization of p53 in 72.3% of freshly isolated peripheral blood mononuclear cells, indicating that the identified *BRAT1* variants do not impair the ATM function (Figure 2h).

In this study, we describe two phenotypic outcomes resulting from a shared genotype at *BRAT1* locus. Although all three patients belong to the mild end of the *BRAT1* phenotypic spectrum, their clinical presentation was completely different. In the first family, the core features shared by the affected brothers include developmental delay, mild-moderate ID, ataxia, and shrunken cerebellum on brain MRI; analogously to previous cases (Mahjoub et al., 2019; Srivastava et al., 2016; Valence et al., 2019), a mild clinical improvement occurred without neuroimaging progression, thus confirming that biallelic *BRAT1* pathogenic variants should be

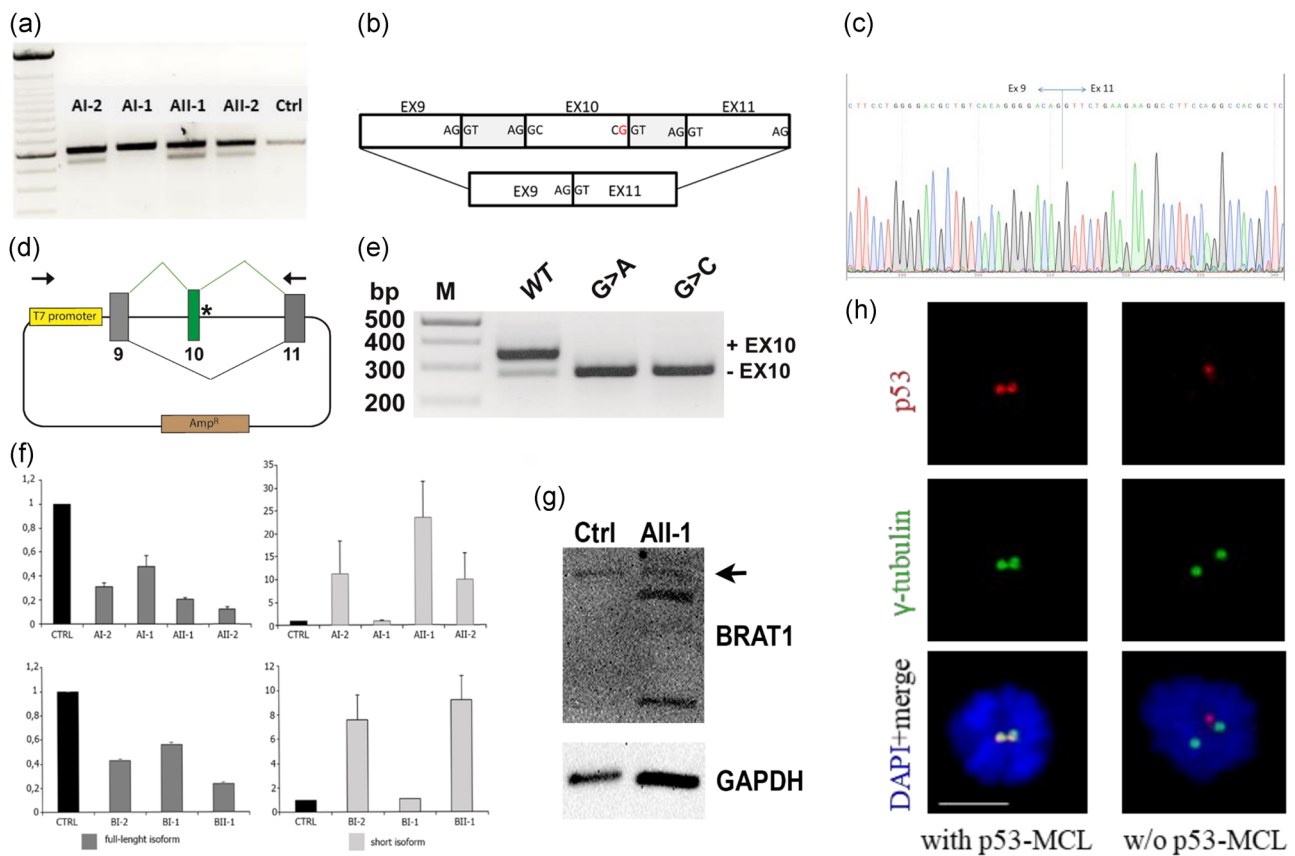


FIGURE 2 Molecular and functional characterization of *BRAT1* variants. (a) Agarose gel electrophoresis of cDNA amplified with primers flanking the supposed deletion breakpoints, showing the ~599 bp expected amplicon (Ctrl and AI-1) and the presence of a lower band in patients AII-1 and AII-2 and their mother (AI-2); (b) schematic partial structure of *BRAT1* transcript (RefSeq NM_152743.3) and alternative splicing isoform (bottom panel) resulting from G to A substitution of the last nucleotide of exon 10 (highlighted in red); (c) Sanger sequence of *BRAT1* cDNA obtained from the alternatively spliced isoform, lacking the 73-bp-long exon 10; and (d) schematic representation of the *BRAT1* minigene. The nucleotide corresponding to the c.1395G>A or c.1395G>C is marked with an asterisk. The genomic sequence of exons 9–11 and flanking introns were cloned in pcDNA3(+) vector; (e) representative RT-PCR analysis of *BRAT1* WT and mutant RNAs isolated from transfected HEK293T cells and amplified using the vector-specific T7 primer and a primer in exon 11; (f) *BRAT1* mRNA levels quantified through qRT-PCR by using primers discriminating the full length and the short transcripts; (g) expression levels of endogenous *BRAT1* protein investigated by western blotting in fibroblasts from patient AII-1; and (h) representative images of p53-MCL in peripheral blood mononuclear cells of patient BII-1. p53 (red) and γ -tubulin (green) were immunostained with specific antibodies by double, indirect immunofluorescence. DNA (blue) was stained with DAPI; 101 mitoses were evaluated to calculate the percentage of p53-MCL: 73 out of 101 mitoses showed colocalization of p53 and γ -tubulin (left panels) while the remaining 28 mitoses showed no colocalization (right panels); p53-MCL is considered normal when the percentage is >70% (scale bar = 5 μ m; \times 100 objective). cDNA, complementary DNA; Ctrl, control; mRNA, messenger RNA; qRT-PCR, quantitative reverse transcription-polymerase chain reaction; WT, wild-type

considered in the differential diagnosis of NPCA. Conversely, the third patient shows the mildest form of NEDCAS so far described, characterized by unexpectedly normal neurodevelopment, adolescence-onset neurological signs, and shrunken cerebellum. Additional previously unreported findings are represented by the reduction of *N*-acetyl aspartate peak on MRS and the evidence for cytoplasmic inclusions in both dermal fibroblasts and myelinated fibers. Such mild phenotypes can partly be explained by the presence of residual *BRAT1* WT protein, as shown by Western blotting. Nevertheless, our laboratory findings do not explain the observed interpatient clinical variability, as expression levels of the full-length and the skipped *BRAT1* transcripts detected in lymphocytes were comparable in both families. Such phenotypic divergence further highlights the complexity of performing genotype–phenotype correlates even

in monogenic recessive disorders, and could rely on the contribution of modifier genes, which still remain to be identified.

Among *BRAT1*-mutated patients, two cases have already been reported with the p.(Thr465=) variant, in homozygous state or in compound heterozygosity with a single amino acid deletion (Burgess et al., 2019; Van Ommeren et al., 2018). In these patients, the synonymous variant originated from the c.1395G>C nucleotide change, while the resulting phenotype was severe and classifiable as RMFSL. Interestingly, the splicing assay performed in HEK293T cells transfected with the G>C mutant minigene gave the same results obtained for the G>A change (Figure 2e), further highlighting the difficulty in reliably predicting clinical outcome from genomic data. As far as we know, no additional variants affecting codon 465 have been reported to date.

Ultrastructural analysis of the skin biopsy, never performed in published cases, suggested possible alterations in mitochondrial homeostasis, in accordance with previous observations. Indeed, two *BRAT1*-mutated patients were reported with reduced cytochrome c oxidase histochemical staining on muscle biopsy and decreased native pyruvate dehydrogenase (PDH) levels in fibroblasts, respectively (Horn et al., 2016; Mahjoub et al., 2019). Moreover, So and Ouchi (2014) showed mitochondrial mislocalization, increased glucose uptake, elevated levels of reactive oxygen species, lower mitochondrial membrane potential, impaired PDH activity, and decreased ATP synthesis in *BRAT1* knockdown HeLa cells, again consistent with a mitochondrial defect. Interestingly, *BRAT1* knockdown cells demonstrate similarities with lymphoblastic cells deficient in ATM protein, which directly interacts with *BRAT1* during DDR. Nevertheless, the ATM-dependent p53-MCL test performed in one of our patients (exploiting a noncanonical ATM signalling) (Prodosmo et al., 2013) failed to show defects in p53 centrosomal localization, suggesting that defective ATM activity does not contribute to the *BRAT1*-related phenotype. This is in agreement with the results from Mahjoub et al. (2019) reporting a normal ATM kinase activity in DDR after exposure of mutant *BRAT1* cells to ionizing radiations.

In the last years, an increasing number of causative genes for NPCA has been reported (e.g., *CACNA1A*, *KCNC3*, *ITPR1*, *SPTBN2*, *PMPCA*), characterized by dominant, recessive, or X-linked inheritance (Bertini et al., 2018). The affected children can present with normal neuroimaging, cerebellar hypoplasia or enlarged cerebellar interfolial spaces without progression over time. In a further subgroup of cases, a progressive enlargement of cerebellar fissures potentially mimicking cerebellar atrophy is observed, in association with clinical improvement. For this reason, a single neuroimaging study may not be able to distinguish NPCA from degenerative progressive cerebellar atrophy, thus making it difficult to make prognostic evaluations. A better understanding of NPCA-associated genes and related phenotypes will help clinicians in reaching the correct diagnosis and better predicting disease outcome. In conclusion, our findings provide evidence for the clinical heterogeneity associated with *BRAT1* variants, and further expand the *BRAT1*-associated spectrum towards the mild end. Mutations in *BRAT1* should be suspected in patients with nonprogressive cerebellar signs, even in the absence of a neurodevelopmental disorder.

ACKNOWLEDGMENTS

This study was supported by grants from the Italian Ministry of Health (Ricerca Finalizzata NET-2013-02356160 to Enrico Bertini, Enza M. Valente, and Gessica Vasco; Ricerca Corrente 2020 to IRCCS Mondino), the European Research Council (Starting Grant 260888 to Enza M. Valente), and the Fondazione Pierfranco e Luisa Mariani (PADAPORT project to Enza M. Valente). The authors are grateful to patients and their families for their cooperation. They would like to thank Dr. Silvia Soddu, Head of Unit of Cellular Networks and Molecular Therapeutic Targets at Regina Elena National Cancer Institute, for supervising functional analyses on ATM activity. Enrico Bertini and Ginevra Zanni are members of the European Reference Network for Rare Neurological Diseases—Project ID No. 739510.

CONFLICT OF INTERESTS

The authors declare that there are no conflict of interests.

AUTHOR CONTRIBUTIONS

Sara Nuovo, Valentina Baglioni, Enza M. Valente, and Vincenzo Leuzzi planned the study. Caterina Caputi, Enrico Bertini, Ginevra Zanni, and Gessica Vasco collected the data and follow-up the patients. Roberta De Mori, Silvia Tardivo, Monia Ginevrino, Alessia Micalizzi, Antonella Casella, Elisa Lorefice, Danila Anello, Manuela Tolve, Lorena Travaglini, and Carla Carducci performed exome sequencing and/or complementary DNA analysis. Donatella Farini and Claudio Sette carried out a splicing reporter minigene assay. Roberta De Mori, Silvia Tardivo, and Giulia Federici conducted functional studies. Laura Masuelli performed ultrastructural analysis of the skin biopsy. Sara Nuovo and Valentina Baglioni wrote the first draft of the manuscript, tables, and figures. All the authors revised the manuscript for important intellectual content and approved the final version.

DATA AVAILABILITY STATEMENT

Clinical and genetic data described in this study are openly available on Global Variome shared Leiden Open Variation Database (<http://www.LOVD.nl>). Variant IDs: #0000382840, #0000382841, #0000382839, #0000382842, #0000709529, and #0000709528. Individual IDs: #00168942, #00168941, and #00325074.

ORCID

Sara Nuovo  <https://orcid.org/0000-0003-1359-5122>
 Valentina Baglioni  <http://orcid.org/0000-0002-5010-8162>
 Roberta De Mori  <http://orcid.org/0000-0002-1197-4308>
 Silvia Tardivo  <http://orcid.org/0000-0001-7623-3407>
 Caterina Caputi  <http://orcid.org/0000-0001-5972-1185>
 Monia Ginevrino  <http://orcid.org/0000-0002-2782-6369>
 Alessia Micalizzi  <http://orcid.org/0000-0001-9927-5781>
 Laura Masuelli  <http://orcid.org/0000-0001-8174-8034>
 Giulia Federici  <http://orcid.org/0000-0002-4684-0270>
 Antonella Casella  <https://orcid.org/0000-0002-1514-2824>
 Elisa Lorefice  <https://orcid.org/0000-0001-8198-6286>
 Manuela Tolve  <https://orcid.org/0000-0003-0263-4325>
 Donatella Farini  <https://orcid.org/0000-0002-1991-3956>
 Enrico Bertini  <http://orcid.org/0000-0001-9276-4590>
 Ginevra Zanni  <https://orcid.org/0000-0002-6367-1843>
 Lorena Travaglini  <https://orcid.org/0000-0003-0142-6516>
 Gessica Vasco  <https://orcid.org/0000-0001-9807-9578>
 Claudio Sette  <https://orcid.org/0000-0003-2864-8266>
 Carla Carducci  <https://orcid.org/0000-0003-2384-1550>
 Enza M. Valente  <https://orcid.org/0000-0002-0600-6820>
 Vincenzo Leuzzi  <https://orcid.org/0000-0002-2314-6139>

REFERENCES

Aglipay, J. A., Martin, S. A., Tawara, H., Lee, S. W., & Ouchi, T. (2006). ATM activation by ionizing radiation requires BRCA1-associated BAAT1. *Journal of Biological Chemistry*, 281(14), 9710–9718. <https://doi.org/10.1074/jbc.M510332200>

- Bertini, E., Zanni, G., & Boltshauser, E. (2018). Nonprogressive congenital ataxias, *Handbook of clinical neurology* (Vol. 155, 1st ed.), pp. 91–103. <https://doi.org/10.1016/B978-0-444-64189-2.00006-8>
- Burgess, R., Wang, S., McTague, A., Boysen, K. E., Yang, X., Zeng, Q., Myers, K. A., Rochtus, A., Trivisano, M., Gill, D., EIMFS, C., Sadleir, L. G., Specchio, N., Guerrini, R., Marini, C., Zhang, Y. H., Mefford, H. C., Kurian, M. A., Poduri, A. H., & Scheffer, I. E. (2019). The genetic landscape of epilepsy of infancy with migrating focal seizures. *Annals of Neurology*, 86(6), 821–831. <https://doi.org/10.1002/ana.25619>
- Colak, F. K., Guleray, N., Azapagasi, E., Yazıcı, M. U., Aksoy, E., & Ceylan, N. (2020). An intronic variant in BRAT1 creates a cryptic splice site, causing epileptic encephalopathy without prominent rigidity. *Acta Neurologica Belgica*, 120(6), 1425–1432. <https://doi.org/10.1007/s13760-020-01513-0>
- Fernández-Jaén, A., Álvarez, S., So, E. Y., Ouchi, T., Jiménez De La Peña, M., Duat, A., Fernández-Mayoralas, D. M., Fernández-Perrone, A. L., Albert, J., & Calleja-Pérez, B. (2016). Mutations in BRAT1 cause autosomal recessive progressive encephalopathy: Report of a Spanish patient. *European Journal of Paediatric Neurology*, 20(3), 421–425. <https://doi.org/10.1016/j.ejpn.2016.02.009>
- Ginevrino, M., Battini, R., Nuovo, S., Simonati, A., Micalizzi, A., Contaldo, I., Serpieri, V., & Valente, E. M. (2020). A novel IRF2BP1 truncating variant is associated with endolysosomal storage. *Molecular Biology Reports*, 47(1), 711–714. <https://doi.org/10.1007/s11033-019-05109-7>
- Hanes, I., Kozenko, M., & Callen, D. J. (2015). Lethal neonatal rigidity and multifocal seizure syndrome—A misnamed disorder? *Pediatric Neurology*, 53(6), 535–540. <https://doi.org/10.1016/j.pediatrneurol.2015.09.002>
- Horn, D., Weschke, B., Knierim, E., Fischer-Zirnsak, B., Stenzel, W., Schuelke, M., & Zemojtel, T. (2016). BRAT1 mutations are associated with infantile epileptic encephalopathy, mitochondrial dysfunction, and survival into childhood. *American Journal of Medical Genetics, Part A*, 170(9), 2274–2281. <https://doi.org/10.1002/ajmg.a.37798>
- Mahjoub, A., Cihlarova, Z., Tétreault, M., MacNeil, L., Sondheimer, N., Caldecott, K. W., Hanzlikova, H., Yoon, G., & Canada, C. (2019). Homozygous pathogenic variant in BRAT1 associated with nonprogressive cerebellar ataxia. *Neurology: Genetics*, 5(5), e359. <https://doi.org/10.1212/NXG.0000000000000359>
- Mastrangelo, M., Alfonsi, C., Screpanti, I., Masuelli, L., Tavazzi, B., Mei, D., Giannotti, F., Guerrini, R., & Leuzzi, V. (2019). Broadening phenotype of adenylosuccinate lyase deficiency: A novel clinical pattern resembling neuronal ceroid lipofuscinosis. *Molecular Genetics and Metabolism Reports*, 21, 100502. <https://doi.org/10.1016/j.ymgmr.2019.100502>
- Mundy, S. A., Krock, B. L., Mao, R., & Shen, J. J. (2016). BRAT1-related disease—identification of a patient without early lethality. *American Journal of Medical Genetics, Part A*, 170(3), 699–702. <https://doi.org/10.1002/ajmg.a.37434>
- Oatts, J. T., Duncan, J. L., Hoyt, C. S., Slavotinek, A. M., & Moore, A. T. (2017). Inner retinal dystrophy in a patient with biallelic sequence variants in BRAT1. *Ophthalmic Genetics*, 38(6), 559–561. <https://doi.org/10.1080/13816810.2017.1290118>
- Pourahmadian, A., Heidari, M., Shojaaaladini Ardakani, H., Noorian, S., & Savad, S. (2020). A novel pathogenic variant of BRAT1 gene causes rigidity and multifocal seizure syndrome, lethal neonatal. *International Journal of Neuroscience*, 131, 875–878. <https://doi.org/10.1080/00207454.2020.1759589>
- Prodosmo, A., De Amicis, A., Nisticò, C., Gabriele, M., Di Rocco, G., Monteonofrio, L., Piane, M., Cundari, E., Chessa, L., & Soddu, S. (2013). P53 centrosomal localization diagnoses ataxia-telangiectasia homozygotes and heterozygotes. *Journal of Clinical Investigation*, 123(3), 1335–1342. <https://doi.org/10.1172/JCI67289>
- Puffenberger, E. G., Jinks, R. N., Sougnez, C., Cibulskis, K., Willert, R. A., Achilly, N. P., Cassidy, R. P., Fiorentini, C. J., Heiken, K. F., Lawrence, J. J., Mahoney, M. H., Miller, C. J., Nair, D. T., Politi, K. A., Worcester, K. N., Setton, R. A., Dipiazza, R., Sherman, E. A., Eastman, J. T., ... Strauss, K. A. (2012). Genetic mapping and exome sequencing identify variants associated with five novel diseases. *PLoS One*, 7(1), e28936. <https://doi.org/10.1371/journal.pone.0028936>
- Scheffer, I. E., Boysen, K. E., Schneider, A. L., Myers, C. T., Mehaffey, M. G., Rochtus, A. M., Yuen, Y. P., Ronen, G. M., Chak, W. K., Gill, D., Poduri, A., & Mefford, H. C. (2020). BRAT1 encephalopathy: A recessive cause of epilepsy of infancy with migrating focal seizures. *Developmental Medicine and Child Neurology*, 62(9), 1096–1099. <https://doi.org/10.1111/dmnc.14428>
- Smith, N. J., Lipsett, J., Dibbens, L. M., & Heron, S. E. (2016). BRAT1-associated neurodegeneration: Intra-familial phenotypic differences in siblings. *American Journal of Medical Genetics, Part A*, 170(11), 3033–3038. <https://doi.org/10.1002/ajmg.a.37853>
- So, E. Y., & Ouchi, T. (2014). BRAT1 deficiency causes increased glucose metabolism and mitochondrial malfunction. *BMC Cancer*, 14, 548. <https://doi.org/10.1186/1471-2407-14-548>
- Srivastava, S., Olson, H. E., Cohen, J. S., Gubbels, C. S., Lincoln, S., Davis, B. T., Shahmirzadi, L., Gupta, S., Picker, J., Yu, T. W., Miller, D. T., Soul, J. S., Poretti, A., & Naidu, S. (2016). BRAT1 mutations present with a spectrum of clinical severity. *American Journal of Medical Genetics, Part A*, 170(9), 2265–2273. <https://doi.org/10.1002/ajmg.a.37783>
- Valence, S., Cochet, E., Rougeot, C., Garel, C., Chantot-Bastaraud, S., Laine, E., Afenjar, A., Barthez, M. A., Bednarek, N., Doummar, D., Faivre, L., Goizet, C., Haye, D., Heron, B., Kemlin, I., Lacombe, D., Milh, M., Moutard, M. L., Riant, F., ... Burglen, L. (2019). Exome sequencing in congenital ataxia identifies two new candidate genes and highlights a pathophysiological link between some congenital ataxias and early infantile epileptic encephalopathies. *Genetics in Medicine*, 21(3), 553–563. <https://doi.org/10.1038/s41436-018-0089-2>
- Van Ommeren, R. H., Gao, A. F., Blaser, S. I., Chitayat, D. A., & Hazrati, L. N. (2018). BRAT1 mutation: The first reported case of Chinese origin and review of the literature. *Journal of Neuropathology and Experimental Neurology*, 77(12), 1071–1078. <https://doi.org/10.1093/jnen/nly093>

SUPPORTING INFORMATION

Additional supporting information may be found in the online version of the article at the publisher's website.

How to cite this article: Nuovo, S., Baglioni, V., De Mori, R., Tardivo, S., Caputi, C., Ginevrino, M., Micalizzi, A., Masuelli, L., Federici, G., Casella, A., Loreface, E., Anello, D., Tolve, M., Farini, D., Bertini, E., Zanni, G., Travaglini, L., Vasco, G., Sette, C., ... Leuzzi, V. (2022). Clinical variability at the mild end of BRAT1-related spectrum: Evidence from two families with genotype–phenotype discordance. *Human Mutation*, 43, 67–73. <https://doi.org/10.1002/humu.24293>